


Proceeding Paper

Effect of Centrifugal Compressor with Influence on Partial Vaned Diffuser [†]

Sathish Sivasubramaniyan, Senbagan Muthusamy, Arulmozhi Kuppusamy, Jensin Joshua, Sarweswaran Rajangam and Seralathan Sivamani * 

Department of Aeronautical Engineering, Hindustan Institute of Technology and Science, Chennai 603 103, Tamil Nadu, India; sathishamg88@gmail.com (S.S.); msenbagan@hindustanuniv.ac.in (S.M.); karulmozhi@hindustanuniv.ac.in (A.K.); jjensin@hindustanuniv.ac.in (J.J.); rswaran@hindustanuniv.ac.in (S.R.)

* Correspondence: siva.seralathan@gmail.com; Tel.: +91-94449-67008

[†] Presented at the International Conference on Processing and Performance of Materials, Chennai, India, 2–3 March 2023.

Abstract: Partial vaned diffusers (PVDs) play a pivotal role in optimizing the performance of turbomachinery systems by efficiently managing fluid flow and pressure differentials. This study delves into the geometric configurations of partial vaned diffusers, examining how variations in vane positioning impact performance. In this study, a PVD is attached either along the hub side (PHVD) or shroud side (PSVD), and a comparison is made between these configurations. Computational fluid dynamics simulations are carried out using ANSYS CFX to elucidate the complex flow patterns within these diffusers for two different mass flow rates, namely 0.30 kg/s and 0.90 kg/s. Flow parameters like pressure, total pressure in the stationary frame, meridional velocity, and velocity are measured. The flow in PSVD is observed to be uniform and the rise in pressure in PSVD is observed to improve by around 4.5% with respect to PHVD. Other flow parameters such as meridional velocity and total pressure are in favor of PSVD.

Keywords: partial vaned diffuser; centrifugal compressor; shroud side; hub side; flow parameters



Citation: Sivasubramaniyan, S.; Muthusamy, S.; Kuppusamy, A.; Joshua, J.; Rajangam, S.; Sivamani, S. Effect of Centrifugal Compressor with Influence on Partial Vaned Diffuser. *Eng. Proc.* **2024**, *61*, 20. <https://doi.org/10.3390/engproc2024061020>

Academic Editors: K. Babu, Anirudh Venkatraman Krishnan, K. Jayakumar and M. Dhananchezian

Published: 31 January 2024



Copyright: © 2024 by the authors. Licensee MDPI, Basel, Switzerland. This article is an open access article distributed under the terms and conditions of the Creative Commons Attribution (CC BY) license (<https://creativecommons.org/licenses/by/4.0/>).

1. Introduction

Applications for centrifugal compressors are numerous. Small turbojet engines, turbochargers, and the oil and gas sectors are some of the applications that use centrifugal compressors. A centrifugal compressor draws energy from a turbine, which is transmitted through the shaft to boost the flow pressure while reducing flow velocity. The impeller, which rotates, and the diffuser, which is fixed, are the two main components of a centrifugal compressor. High-velocity flow enters axially through the eye of the centrifugal compressor and comes out of the impeller in a radial direction. As the flow moves through the diffuser passage, the diffuser's role is to transform the remaining kinetic energy into pressure energy [1].

A numerical investigation was conducted by Shuai Li et al. [2] to study the impact of various diffuser shapes on the aerodynamic performance and flow stability of a stage involving a centrifugal compressor (mass flow coefficient 0.196). A shroud-side partial vaned diffuser exhibited better adaptability than a standard full-height vaned diffuser, whose performance rapidly deteriorated. The formation of vortices at the diffuser's leading edge was inhibited by the shroud-side partial vaned diffuser. As a result, it enhanced the stage's flow stability at low mass flow rates and lessened the flow loss inside the stage. Issac et al. [3] examined the performance of a low-speed centrifugal compressor through experimentation with diffuser vane heights and positions. The diffuser width and diffuser vane height were systematically changed. The compressor performance was minimally affected by the position of the partial vane on the shroud/hub. The compressor performed noticeably better when the hub's partial vanes were fastened and the shroud was stowed at

half its normal spacing. The impact of two different types of partial vaned diffusers on the compressor stage performance was numerically examined. The hub-side vaned diffuser had its partial vanes fastened onto the hub's wall, while the shroud-side vaned diffuser had its partial vanes fixed onto the shroud's wall. The findings demonstrate that the hub-side vaned diffuser was not as effective as the shroud-side vaned diffuser [4].

The influence of impeller–diffuser interactions on an impeller's performance at a particular tip clearance was performed using CFD code ANSYS CFX [5]. The hub vaned diffuser's stage efficiency peaked at 0.5 h/b ratios along with lower flow rates. The operating range of the hub vaned diffusers was greater than that of a vaned diffuser. The shroud vaned diffuser performed better than the hub vaned diffuser for a vane of equivalent height [6]. The diffuser vane angle affected the operating ranges of the compressor, and variable inlet guide vane-casing treatment was required to attain the widest operating range [7]. In a conventional diffuser, flow separation was caused by the pressure differential along the vane's suction surface near the vane's leading edge [8]. Moreover, the stability of the centrifugal compressor was significantly influenced by the way the diffuser operated in a compressor stage [9]. A series of tests were conducted using vaned diffusers and vaneless diffusers at high pressure ratios. The vaned diffuser gave a strong pressure rise in accordance with the one-dimensional flow theory and improved the compressor stage stability. Airfoil-shaped low-solidity diffusers outperformed the flat-plate and circular arc profiles in terms of performance [10]. The compressor operated more effectively when partial vanes were connected to the shroud and the hub was staggered at half-space [11]. Furthermore, the compressor's performance was affected by the inlet configuration and inlet flow structure [12].

In the low-volume range, a hub vaned diffuser with a height-to-breadth ratio of 0.3 and a vaneless diffuser in the large-volume range gave higher mass-averaged static pressure coefficients [13]. While the pressure ratios rose at low rotational speeds, they decreased at high rotational speeds. The diffuser designed with a width ratio of 0.854 performed better [14]. Experimental research on the impact of impeller width on the operation of low-solidity vaned diffusers in centrifugal compressor stages was carried out by Hu et al. [15]. Experiments were conducted to see how the vane setting angle affected the diffuser's performance and stage characteristics because of the circumferential distortion of the volute [16]. To obtain an acceptable stage performance, the diffuser must be configured properly with respect to the impeller. Diffuser setting angles that were smaller than the impeller outlet flow angles offered a wide operating range [17].

Low-solidity vaned diffusers are considered to have a wider operating range than vaned diffusers. The static pressure rise for the vaned diffuser was significantly smaller at high flow coefficients because of the high incidence on the vane leading edge [18]. An experimental analysis was carried out by Yanjie Zhao et al. [19] to compare the performances of conventional and reduced-solidity diffuser systems in a centrifugal compressor. A steady-state compressor stage simulation with the impeller and diffuser having three different inlets was performed to understand the influence of each inlet type on the compressor performance. As the flow from the bent intake exhibited circumferential and radial distortions that were not axisymmetric, the diffuser and the impeller were modeled using 360-degree channels in their entirety [20].

Based on literature reviews, it is understood that partial vaned diffusers give a better static pressure recovery and pressure rise. Therefore, the objective of this work is to numerically examine a compressor stage comprising an impeller with a partial vaned diffuser at different mass flow rates, and the flow parameters are examined. The numerical investigation is carried out using CFD code, ANSYS CFX and the positioning of the partial vanes is changed by attaching them to the hub and shroud sides, respectively.

2. Computational Methodology

The intention is to reduce the flow velocity and increase the pressure across the stage outlet by modifying the positions of the partial vaned diffuser (PVD), i.e., attachment

of the PVD along the hub side as well as the attachment of PVD to the shroud side. A schematic arrangement of the centrifugal compressor with a partial vaned diffuser is shown in Figure 1a. The numerical investigations are carried out on a centrifugal compressor stage for two different mass flow rates, namely 0.30 kg/s and 0.90 kg/s. Table 1 lists the geometric details of the diffusers [1].

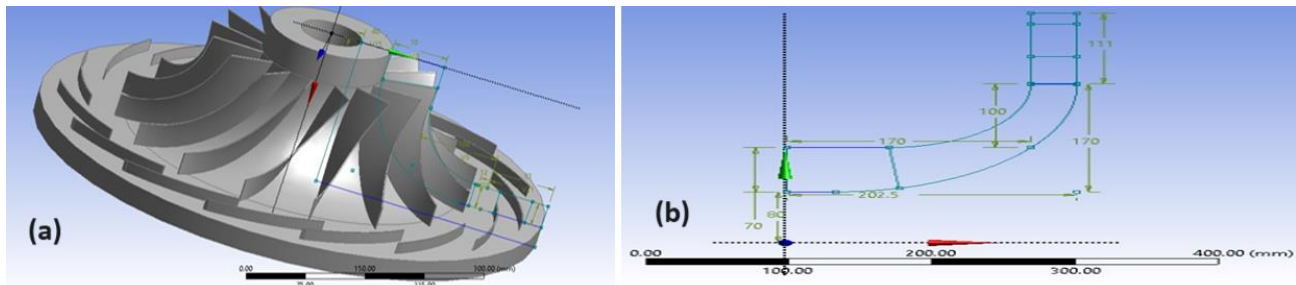


Figure 1. (a) Centrifugal compressor stage; (b) Geometric dimensional details [1].

Table 1. Geometric details of the diffusers [1].

Parameter	Value
Vane solidity (σ)	1.4
Number of vanes (z)	15
Width (b)	32.5 mm
Stagger angle (γ)	16.15°
Vane chord (ch)	163 mm
Vane radius (r_b)	596.58 mm
Outlet vane angle (α_4)	35°
Inlet vane angle (α_3)	24°
Vane outlet radius (r_4)	361 mm
Vane inlet radius (r_3)	280 mm

The hub radius of the centrifugal compressor is 80 mm, and the shroud radius is 150 mm. The outlet radius is 250 mm and the outlet width is 35 mm. There are 15 diffuser vanes and 16 impeller blades in the centrifugal compressor stage. Figure 1b depicts the centrifugal compressor geometry [1]. Using ANSYS Blade Modeler, two geometric models are created by widening the space between the hub and shroud [21]. In steady-state simulations, investigations are performed for two different mass flow rates. This study is performed using the for-profit application, ANSYS CFX. The volume mesh used in the simulation is a mathematical description of a geometry-related space problem. The mesh object, in turn, allows for the appropriate arrangement of vertices, faces, and Cartesian or curvilinear cellular grids. The centrifugal impeller contains 117,872 elements and 242,913 nodes, whereas the partial hub vaned diffuser has 263,312 nodes and 146,476 elements. Similarly, the partial shroud vaned diffuser has 284,917 nodes and 178,086 elements. Unstructured tetrahedral mesh is generated for the whole computational domain using ANSYS ICEM-CFD (<https://www.ansys.com/training-center/course-catalog/fluids/introduction-to-ansys-icem-cfd>, accessed on 21 January 2024).

The centrifugal compressor stage comprising an impeller and a partial vaned diffuser is treated with a single-passage approach for the sake of conserving the computational resources. The boundaries involved in this study are hub, shroud, impeller blades, partial vaned diffuser, inlet, and outlet. At the inlet, a total pressure of 1 atm is specified, whereas mass flow rate is defined as the exit boundary condition. The impeller blades and diffuser vanes are defined as walls with no-slip conditions. Boundary conditions for the centrifugal compressor stage are described using ANSYS CFX PRE. Rotational periodicity is defined along the sides of the computational domain. The centrifugal compressor's shroud and hub have a boundary condition that is defined as a wall with no-slip conditions. The

diffuser is supposed to be a stationary component, while the impeller rotates. Therefore, an interface is introduced between the rotating and stationary domain using the frozen rotor interface concept as the whole computational domain is defined as a rotating domain. The diffuser is defined with a counter-rotating boundary condition that makes it stationary. Figure 2 displays the boundary conditions. The simulations are carried out using ANSYS CFX. A k-omega turbulence model with shear stress transport is chosen to achieve the closure for the Reynolds Averaged Navier's Stokes equations. The steady-state simulation is allowed to be solved in ANSYS Solver until all the residual values become converged. The convergence criteria for the simulations are set as 1×10^{-3} .

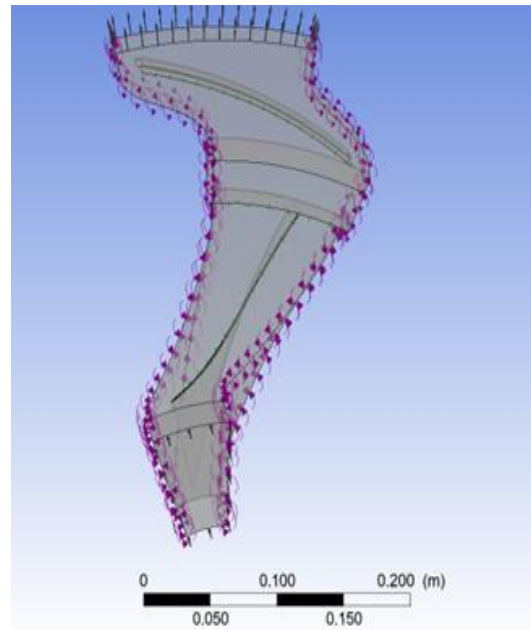


Figure 2. Boundary conditions.

3. Results and Discussion

A turbo surface with constant spans $S = 0.10, 0.50,$ and 0.95 is generated for post-processing the results using ANSYS CFX POST for both the hub-side partial vaned diffuser and the shroud-side partial vaned diffusers. The flow parameters for the hub-side-located partial vaned diffuser (PHVD) and the shroud-side-located partial vaned diffuser (PSVD) are compared and discussed here.

Figure 3 shows the pressure variations from hub to shroud ($S = 0.1$ to 0.95) for the partial vaned diffuser located on the hub side (PHVD). The pressure across the PSVD is higher in comparison with the PHVD. In PSVDs, the pressure increase pattern is consistent across the spans, whereas it varies slightly in PHVDs. In PSVDs, the impeller is more responsible for the increase in pressure than in PHVDs. Moreover, there are no flow interruptions and a clear pressure-rising pattern is observed. At span $S = 0.95$, the pressure is high for both diffuser configurations.

Figure 4 shows the variations in total pressure ($S = 0.1$ to 0.95) for the shroud-side-located partial vaned diffuser at a mass flow rate of 0.30 kg/s. Flow separation across diffusers is caused by the presence of diffuser vanes. There is a flow disturbance caused by the flow separation in the PHVD at spans $S = 0.1$ and 0.5 , as well as in the PSVD at span $S = 0.5$. The overall total pressure across the diffuser in the PHVD configuration is greater at spans $S = 0.1$ and 0.95 in comparison with the PSVD. Even though the total pressure at the diffuser's inlet is higher in the PSVD, the flow separation causes the total pressure at the diffuser's exit to decrease slightly less in the PSVD in comparison with the PHVD. Total pressure distribution differs along the diffusers, except for the PSVD at spans $S = 0.1$ and 0.95 , where it is consistently constant.

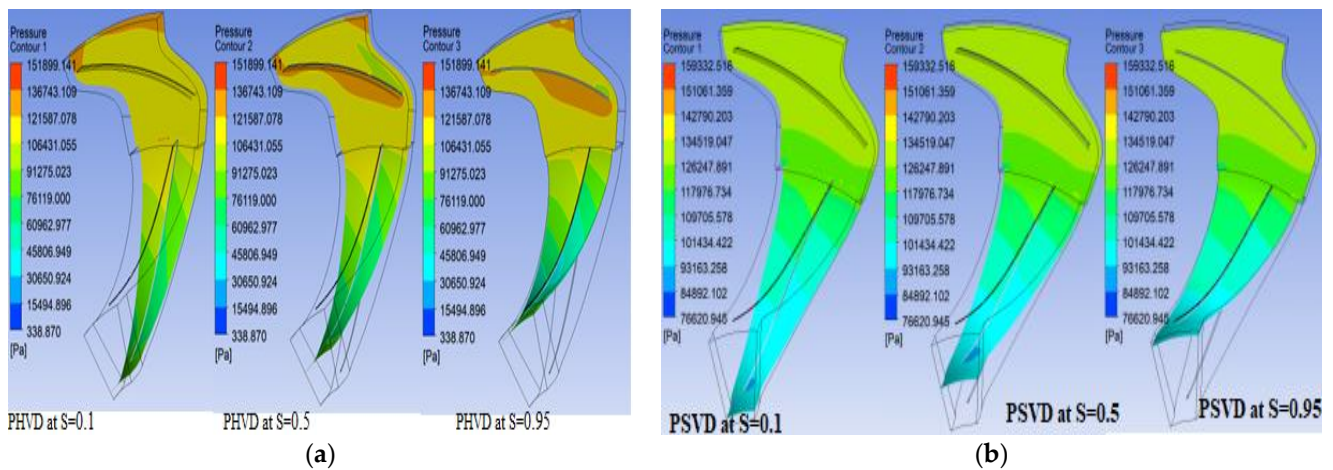


Figure 3. Pressure variations from hub to shroud for (a) PHVD and (b) PSVD.

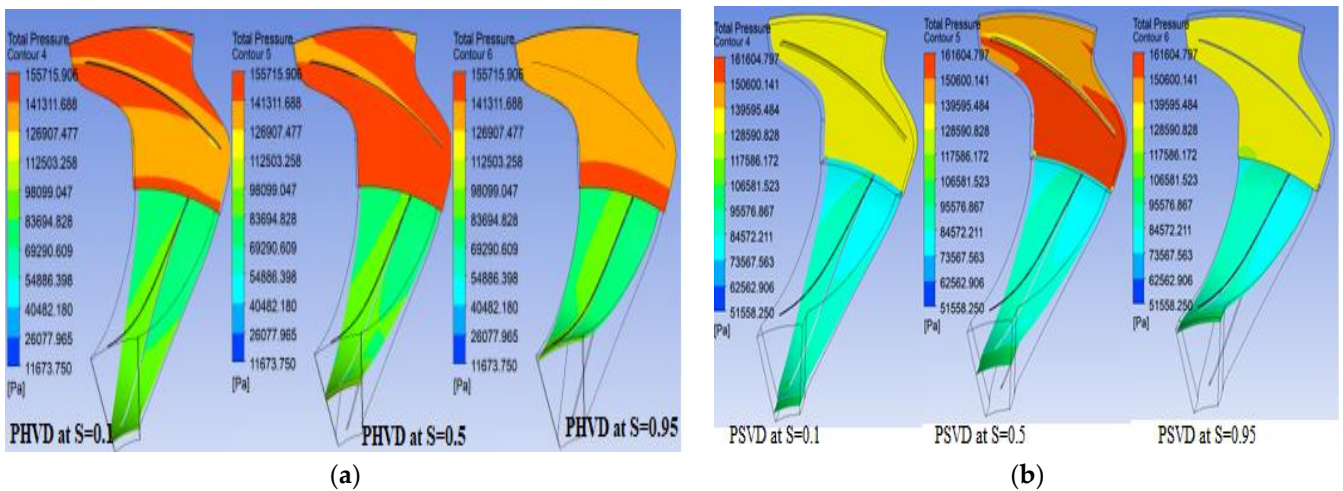


Figure 4. Total pressure variations from hub to shroud for (a) PHVD and (b) PSVD.

Figure 5 shows the variations in absolute velocity for the partial vane located along the shroud in the partial vaned diffuser for a mass flow rate of 0.30 kg/s. In the diffusers, there is a significant flow separation at mid-span $S = 0.5$. When compared to the PHVD, the velocity is lower in the PSVD configuration. At mid-span, the flow velocity is higher across the diffusers, while at span $S = 0.95$, the flow velocity is low. Disoriented velocity variations are more prevalent in the diffusers at span $S = 0.5$. Impeller crossflow velocities vary, except for those with span $S = 0.1$, where they are nearly the same. In the PSVD, the flow separation is primarily around the diffuser’s outer edge. However, it can be found inside the diffusers in the PHVD configuration.

Figure 6 illustrates the velocity vector variations for the partial vaned diffuser configurations at a mass flow rate of 0.30 kg/s. When compared to the PHVD, the PSVD has a lower flow velocity. At mid-span and span location $S = 0.95$, the velocity of flow is high and low, respectively. All diffusers in the PHVD have an identical velocity vector at the outlets across all spans. The velocity is greater at span $S = 0.5$, but it decreases toward the diffuser outlet. The velocity vectors in diffusers and impellers at span $S = 0.1$ are identical. Between spans $S = 0.1$ and 0.95 , the velocity vector stays constant throughout the PSVD.

Figure 7 depicts the variations in the velocity across the diffusers for a mass flow rate of 0.9 kg/s. At $S = 0.1$, close to the diffuser walls, both the PSVD and PHVD configurations experience flow separation. The PSVD, at $S = 0.95$, shows a little drop despite the high-velocity flow present in each of the spans. In comparison with the impeller, the flow through the PSVD within the diffuser is observed to be uniform.

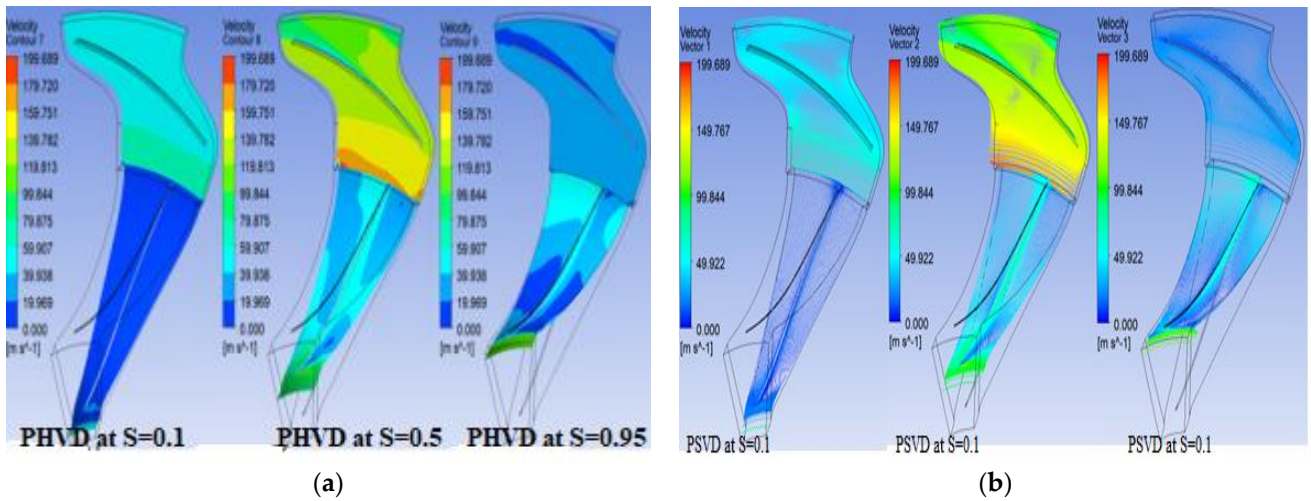


Figure 5. Velocity variations from hub to shroud for (a) PHVD and (b) PSVD.

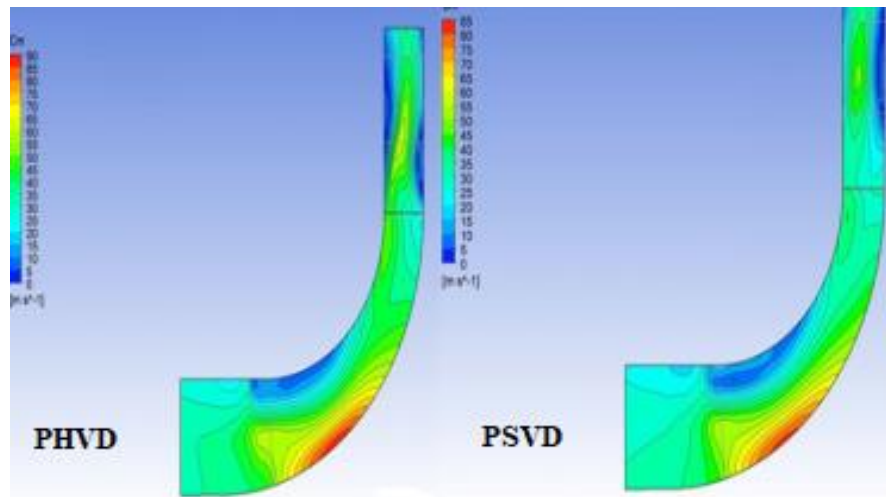


Figure 6. Velocity vectors.

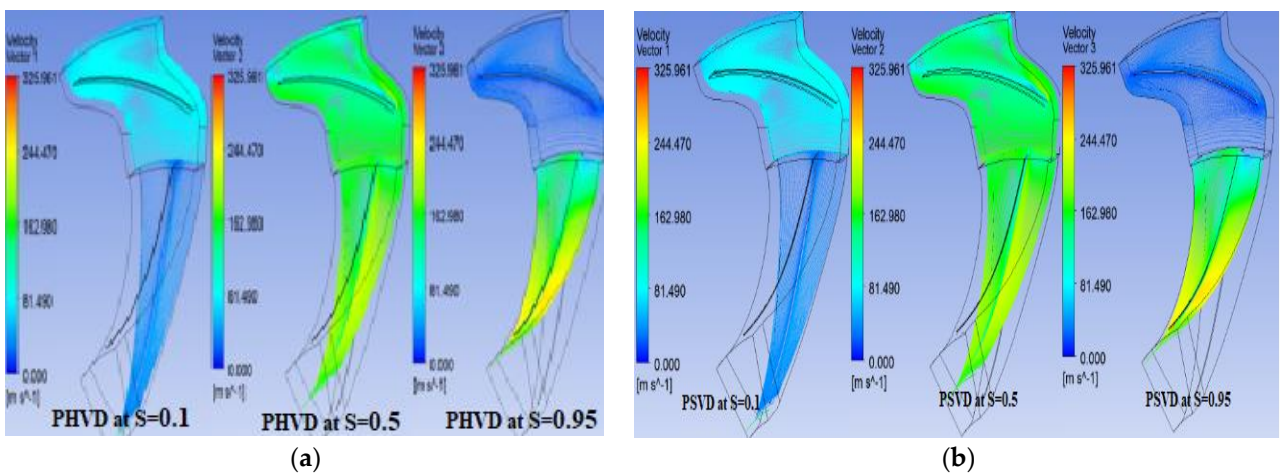


Figure 7. Velocity distribution across diffuser for (a) PHVD and (b) PSVD at mass flow rate 0.9 kg/s.

Figure 8 shows the variations in meridional velocity for the partial vaned diffusers at a mass flow rate of 0.30 kg/s. As can be seen in the Figure, a flow separation within the

impeller is observed along the hub side. Meridional velocity is higher across the PHVD than in the PSVD. There is a flow separation in the diffuser of the PHVD along the shroud and flow separation in the diffuser of the PSVD at both the hub and shroud sides. The velocity is high along the impeller, but it decreases as the flow progresses toward the inlet of the diffuser due to diffusion. The maximum velocity observed in the PHVD is 90 m/s, whereas it is 85 m/s in other locations. At the diffuser outlet, the velocity of the PSVD is lower compared to the PHVD.

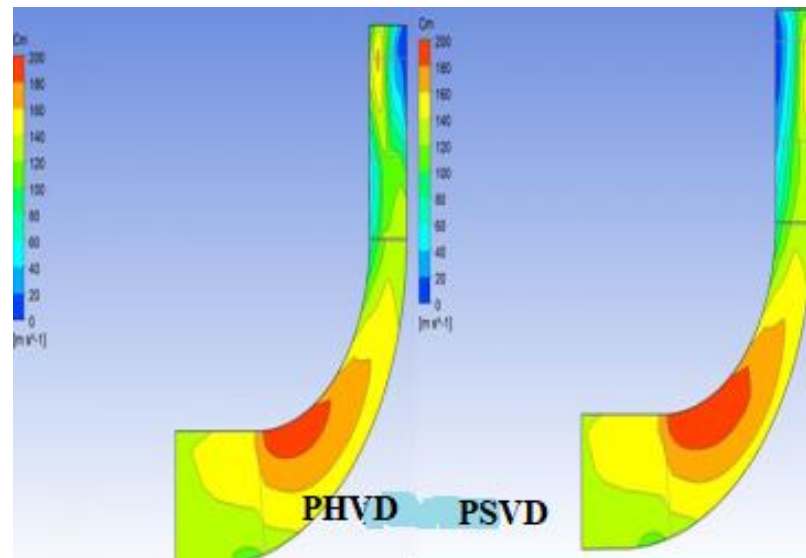


Figure 8. Meridional velocity.

4. Conclusions

A computational study was carried out on a centrifugal compressor stage with a partial vaned diffuser. The location of the partial vane was considered on the hub side and on the shroud side. Based on this study, the following points are concluded.

At a higher mass flow rate, the shroud-side-located partial vaned diffuser operates well. The average pressure rise at the midspan location of the PSVD is higher compared to the PHVD. The flow in the PSVD is observed to be uniform and the rise in pressure in the PSVD is observed to be better by around 4.5% with respect to the PHVD. With flow parameter aspects, the shroud-side-located partial vaned diffuser outperforms the hub-side-located partial vaned diffuser. The shroud-side-located partial vaned diffuser achieves a higher pressure rise than the hub-side-located partial vaned diffuser. It can be concluded that the shroud-side-located partial vaned diffuser performs better than the hub-side-located partial vaned diffuser.

Author Contributions: Conceptualization, S.S. (Sathish Sivasubramaniyan) and J.J.; methodology, S.M. and S.R.; software, S.S. (Seralathan Sivamani); formal analysis, S.S. (Seralathan Sivamani); investigation, S.S. (Seralathan Sivamani); data curation, A.K.; writing—original draft preparation, S.S. (Seralathan Sivamani); writing—review and editing, S.S. (Seralathan Sivamani); supervision, S.S. (Seralathan Sivamani). All authors have read and agreed to the published version of the manuscript.

Funding: This research received no external funding.

Institutional Review Board Statement: Not applicable.

Informed Consent Statement: Not applicable.

Data Availability Statement: Data will be made available on request.

Conflicts of Interest: The authors declare no conflict of interest.

References

1. Gunadal, S.M.; Govardhan, M. Performance Improvement of a Centrifugal Compressor Using Partial Vaned Diffusers. *Int. J. Fluid Mach. Syst.* **2020**, *13*, 177–189. [[CrossRef](#)]
2. Li, S.; Liu, Y.; Li, H.; Omid, M. Numerical study of the improvement in stability and performance by use of a partial vaned diffuser for a centrifugal compressor stage. *Appl. Sci.* **2021**, *11*, 6980. [[CrossRef](#)]
3. Issac, J.M.; Sitaram, N.; Govardhan, M. Effect of diffuser vane height and position on the performance of a centrifugal compressor. *Proc. Inst. Mech. Eng. Part A J. Power Energy* **2004**, *218*, 647–654. [[CrossRef](#)]
4. Sathish, S.; Seralathan, S.; Balaji, G.; Kumar, N.; Madhu, G.; Muthuram, A. Aerodynamic Analysis of Supersonic Flow through a Dual Bell Nozzle using CFD. In Proceedings of the 2022 International Conference on Power, Energy, Control and Transmission Systems (ICPECTS), Chennai, India, 8–9 December 2022; IEEE: Piscataway, NJ, USA, 2022; pp. 1–5.
5. Nguyen, D.A.; Ma, S.B.; Kim, S.; Kim, J.H. Hydrodynamic optimization of the impeller and diffuser vane of an axial-flow pump. *J. Mech. Sci. Technol.* **2023**, *37*, 1263–1278. [[CrossRef](#)]
6. Sathish, S.; Seralathan, S.; Ch, M.S.N.; Rizwan, V.M.; Varma, U.P.; Kumar, K. Influence of converging conical hole angles on jet impingement blade cooling of gas turbine blade leading edge. *AIP Conf. Proc.* **2022**, *2385*, 120003.
7. Ubben, S.; Niehuis, R. Experimental investigation of the diffuser vane clearance effect in a centrifugal compressor stage with adjustable diffuser geometry—Part I: Compressor performance analysis. *J. Turbo Mach.* **2015**, *137*, 031003. [[CrossRef](#)]
8. Seralathan, S.; Kumar, P.S.; Singh, S.; Raj, R.; Sathish, S. Numerical analysis of the one-stage and two-stage helical Savonius vertical axis wind turbine. *AIP Conf. Proc.* **2022**, *2385*, 120005.
9. Ohta, Y.; Goto, T.; Ota, E. Effects of tapered diffuser vane on the flow field and noise of a centrifugal compressor. *J. Therm. Sci.* **2007**, *16*, 301–308. [[CrossRef](#)]
10. Kawashima, D.; Kanemoto, T.; Sakoda, K.; Wada, A.; Hara, T. Matching diffuser vane with return vane installed in multistage centrifugal pump. *Int. J. Fluid Mach. Syst.* **2008**, *1*, 86–91. [[CrossRef](#)]
11. Muthuram, A.; Kavikumar, K.; Seralathan, S.; Sathish, S.; Anita, M. Computational Investigation of Jet Mixing Enhancement by CD Nozzle with Arc Tabs. In Proceedings of the 2022 International Conference on Power, Energy, Control and Transmission Systems (ICPECTS), Chennai, India, 8–9 December 2022; IEEE: Piscataway, NJ, USA, 2022; pp. 1–6.
12. Fu, L.; Zhu, X.; Jiang, W.; Li, G. Numerical investigation on influence of diffuser vane height of centrifugal pump. *Int. Commun. Heat Mass Transf.* **2017**, *82*, 114–124. [[CrossRef](#)]
13. Goto, T.; Ohmoto, E.; Ohta, Y.; Ota, E. Noise reduction and surge margin improvement using tapered diffuser vane in a centrifugal compressor. *J. Therm. Sci.* **2010**, *19*, 21–25. [[CrossRef](#)]
14. Reddy, T.C.S.; Ramana Murty, G.V.; Prasad, M.V.S.S.M. Effect of diffuser vane shape on the performance of a centrifugal compressor stage. *J. Therm. Sci.* **2014**, *23*, 127–132. [[CrossRef](#)]
15. Hu, C.; Yang, C. Numerical modeling of the dynamic unsteadiness with global mode decomposition approach in a high-speed compressor with abnormal diffuser vane. *Proc. Inst. Mech. Eng. Part D J. Automob. Eng.* **2023**, *237*, 1855–1867. [[CrossRef](#)]
16. Seralathan, S.; Hariram, V.; Sathishkumar, M.; Vasudev, K.L. Comparison of Hydrodynamic Characteristics of Porous and Solid Square Cylinder at Low Reynolds Number Using CFD. In *Recent Advances in Energy Technologies: Select Proceedings of ICENT 2021*; Springer Nature: Singapore, 2022; pp. 273–285.
17. Seralathan, S.; Mhatre, P.S.; Vijay, D.V.; Kumari, A.M.; Hariram, V. CFD Analysis of S-Duct with Varying Area Distributions. *Int. J. Veh. Struct. Syst. (IJVSS)* **2021**, *13*, 12–21. [[CrossRef](#)]
18. Engeda, A.; Kim, Y.; Aungier, R.; Direnzi, G. The Inlet Flow Structure of a Centrifugal Compressor Stage and Its Influence on the Compressor Performance. *J. Fluids Eng.* **2003**, *125*, 779–785. [[CrossRef](#)]
19. Zhao, Y.; Li, J. Study of the flow characteristics in the multi row vaned diffusers of centrifugal compressor stage. *Adv. Mech. Eng.* **2008**, *10*, 1687814018799608. [[CrossRef](#)]
20. Liu, R.; Xu, Z. Numerical investigation of a high-speed centrifugal compressor with hub vaned diffusers. *Inst. Mech. Eng.* **2004**, *218*, 155–169. [[CrossRef](#)]
21. Anish, S.; Sitaram, N.; Kim, H.D. A Numerical Study of the Unsteady Interaction Effects on Diffuser Performance in a Centrifugal Compressor. *J. Turbomach.* **2014**, *136*, 011012. [[CrossRef](#)]

Disclaimer/Publisher’s Note: The statements, opinions and data contained in all publications are solely those of the individual author(s) and contributor(s) and not of MDPI and/or the editor(s). MDPI and/or the editor(s) disclaim responsibility for any injury to people or property resulting from any ideas, methods, instructions or products referred to in the content.